Electronic Journal of General Medicine
2024, 21(3), em590
e-ISSN: 2516-3507
https://www.ejgm.co.uk/

MODESTUM

Original Article

OPEN ACCESS

Carrageenan-amino acid interaction as a tool for understanding atherosclerotic process initiation

Paula Monique Chiconi de Picoli [1], Tatiane Araújo Soares [1], Adriano Marques Gonçalves [2], Eliane Trovatti [1]*

[1] University of Araraquara, Araraquara, SP, BRAZIL
[2] College of Veterinary Medicine and Animal Science, University of São Paulo, São Paulo, SP, BRAZIL
***Corresponding Author:** elianetrov@yahoo.com.br

Citation: Chiconi de Picoli PM, Araújo Soares T, Marques Gonçalves A, Trovatti E. Carrageenan-amino acid interaction as a tool for understanding atherosclerotic process initiation. Electron J Gen Med. 2024;21(3):em590. https://doi.org/10.29333/ejgm/14652

ARTICLE INFO

Received: 09 Dec. 2023

Accepted: 05 May 2024

ABSTRACT

Atherosclerosis is the primary trigger for severe pathologies. The atherosclerotic inflammatory process is well known after low-density lipoprotein (LDL) adhesion in blood vessel walls, however, limited information exists regarding LDL penetration into subendothelial layers. Here, we propose for the first time, to the best of our knowledge, the pathway for the initial trajectory of the lipid molecules internalization into the arterial endothelial tissue. The investigation shows a computational model analyzing molecules involved in the atherosclerotic process, specifically LDL and molecules of the vascular endothelium. The theoretical model was experimentally tested using carrageenan to simulate the anionic counterparts of vascular tissue and amino acids from apolipoprotein B-100. The molecular interactions were analyzed by conductimetric titration, FTIR, and rheology. The computational model identified potential amino acids involved in the process, and the experimental results demonstrated the interaction between lysine and polymer, as the mechanism of adhesion, confirming the model.

Keywords: atherosclerosis, apolipoprotein B-100, lysine, low-density lipoprotein, dermatan sulfate

INTRODUCTION

Atherosclerosis is a pathology characterized by the gradual accumulation of fatty plaques in arterial endothelial tissue over years [1-5]. If undiagnosed, the growth of lipid plaques interrupts the blood flow, leading the affected area to necrosis [6, 7]. Atherosclerosis affects 10% of the global population [8, 9] and is the primary trigger for pathologies such as acute myocardial infarction, ischemic stroke and peripheral arterial disease (PAD), among others [10-13]. Acute myocardial infarction accounts for 15 million annual deaths worldwide [14], with 80% occurring within the first 24 hours after disease manifestation [15]. Ischemic stroke is a leading cause of death and neurological sequelae [16, 17], with a 40% mortality rate within the first year of disease onset. Diagnosis and treatment within the first 4.5 hours are crucial, as delayed intervention often results in irreversible damage [18]. PAD is the major predictor of amputations, with 87% of global amputations attributed to this pathology. Early diagnosis is challenging, as 70% of cases are asymptomatic, leading to clinical progression and increased amputation rates [19].

Atherosclerosis starts with vascular endothelial dysfunction, predominantly in areas of arterial bifurcations, branches, or angulations [20]. In these sites the blood flow generate turbulence because of the anatomy, increasing the chances of tissue injuries [21]. The literature provides a detailed description of the atherosclerotic process after low-density lipoprotein (LDL) molecules adhere to the internal blood vessel walls generating the atheroma plaques [22-24]. In short, atherosclerosis is an inflammatory process in specific artery regions [25-27]. Injured endothelial cells express cytokines and chemokines [28-30] such as tumor necrosis factor-alpha and interleukins 1, 6, and 8 [31-33], attracting immune mediators like monocytes and T cells to the arterial endothelial surface through selectin and integrin expression [34-37]. The injured endothelial surface exhibits negative charges from proteoglycans [38], molecules based on the proteinaceous core of aggrecan. Anionic glycosaminoglycan chains, dermatan sulfate, and chondroitin sulfate covalently bind to the protein core through serine residues in the central protein skeleton [39-41]. In this sense, LDL molecules in the bloodstream are attracted by dermatan sulfate and chondroitin sulfate molecules on the surfaces of injured arteries [42]. Additionally, LDL molecules adhering to arterial tissue are endocytosed, along with macronutrients, by endothelial cells, in an endocytosis process independent of LDL receptors [43], which are not expressed because there is no need of LDL molecules for cell metabolism at that moment. These LDL molecules are then released into the extracellular space in the subendothelial layer inside the arterial vessel wall, where they are attracted by glycosaminoglycans at the cell interstices [44]. Besides glycosaminoglycans, elastin and collagen fibers at the subendothelial layer, also contribute to keep LDL in artery walls [45, 46]. LDL molecules are oxidized by myeloperoxidase and NADPH oxidase enzymes and oxygen reactive species at the subendothelial layer [47-50]. The oxidative process leads LDL molecules to be recognized by

scavenger receptors at the surface of macrophages [51-54]. Macrophages remove LDL molecules from artery walls [55]. Thus, oxidized LDL molecules are identified, phagocytosed by macrophages, and transformed into foam cells [56-59]. Foam cell aggregation results in atheroma plaques [60-62].

As described above, the inflammatory process and the formation of the atheroma plaque after internalization of LDL are very well described in the literature, however, little information is available about the process by which LDL molecules penetrate the endothelial layers. For internalization, LDL certainly interacts with the molecules at the surface of the endothelial cells, a crucial process that needs to be deeply understood to elucidate the beginning of plaque formation.

Hence, based on the information from the literature, this work aims to contribute to elucidating the starting point of the atherosclerotic process, namely, the initial steps of the molecular interactions between LDL molecules and the vessel walls. In this sense, the chemical structure of LDL and the surface molecules of the endothelial cells were studied. Then, we have proposed a lipid adhesion model, which predicts the electrostatic interaction between LDL molecules and endothelial tissue cells. The model anticipates that this interaction only occurs in injured tissue after the initiation of an inflammatory process, and to the best of our knowledge, it is not described in the literature. The model employed the polymer carrageenan and the primary amino acids lysine, serine or arginine. Carrageenan displays a pendent sulphate group at its surface and was used to simulate the pendent sulphate group from dermatan sulphate available at the surface of the epithelial cells. It was also used because it displays only sulphate and hydroxyl groups in its structure, available for hydrogen bonds or electrostatic interactions. The primary amino acids were those available at the surface of apolipoprotein B-100. The model aims to predict the interfacial adhesion between them, possibly by electrostatic interactions, which can lead to the adhesion of LDL to the surface of the epithelial cells.

METHODOLOGY

Molecular Modeling & Docking

The protonation state of dermatan sulphate was estimated at 7.4 pH, using MarvinSketch (v.21.2) software. Dermatan sulphate was constructed with Discovery Studio Visualizer (v.20.1) [63]. The tridimensional structures were optimized using the semi-empirical method PM7 in MOPAC (v.2016) [64] with graphical interface of Mercury CSD software (v2020.1) [65]. The optimization commands MMOK, XYZ and CHARGE (depending on the charge of each molecule at 7.4 pH).

Since APOB-100 protein does not have a solved 3D structure, I-TASSER was used to model a 355 amino acid length sequence of the protein structure. The chosen region was based on studies pointing to residues important for the apo-B100 interaction. The 355 amino acid sequence was retrieved from the apo-B100 human protein (Uniprot ID P04114) from residues 3186 to 3540.

For docking studies hydrogen atoms were added to .pdb file with GOLD software (v.2020.1). The same software was used to perform the rigid docking, using L3391 coordinates of the modeled structure as the center of the 10 Å search radius. The method was applied using 100 runs, and GoldScore function.

Conductimetric Titration

For the conductimetric titrations, solutions of the amino acids lysine, arginine, and serine (1 mM) were first prepared at room temperature, along with the carrageenan polymeric solution (0.1 mol/L) at 60 °C. Subsequently, the pH of the solutions was adjusted to 7. A 3 mL aliquot of the carrageenan polymeric solution was placed in a beaker. A conductimetric cell (Analyzer 650MA conductometer) was immersed in the solution for analysis. The polymeric solution was titrated with different amino acids–lysine, arginine, and serine—under constant stirring, with the conductance value recorded after each addition of titrants at 25 °C. Following each addition, a waiting period of approximately one minute was observed for stabilization before each reading.

Chemical Characterization by FTIR

The chemical characterization of the lysine, arginine, and serine amino acid solutions, carrageenan polymer, and carrageenan-amino acid solutions was performed using FTIR (with ATR accessory) on a Perkin Elmer Spectrum 100 spectrometer at a resolution of 4 cm^{-1}, with 16 scans in the range of 4,000 to 600 cm^{-1}. The amino acid solutions (lysine, arginine, and serine) and carrageenan solution used for FTIR analysis were the same as those prepared for the conductimetric titration analysis. Carrageenan-lysine, carrageenan-arginine, and carrageenan-serine solutions were prepared by mixing 0.5 mL of the carrageenan solution with 0.5 mL of the amino acid solutions at room temperature. Aliquots of the carrageenan-amino acid solutions were dried in an oven at 45 °C, and the analysis was then carried on the dried samples.

Rheology

The samples used in the rheological analysis, polymeric solution, and polymeric-amino acid solutions, were the same solutions prepared and used in the conductimetric titration and FTIR analysis. Rheological analyses of the carrageenan, carrageenan-lysine, carrageenan-arginine, and carrageenan-serine samples were performed using an Anton Paar MCR92 rheometer. To ensure result accuracy, a specific configuration was adopted, employing a 50 mm parallel plate geometry during the tests. The main objective was to evaluate viscosity concerning the reaction time of the samples under study. To maintain test consistency and uniformity, the following experimental parameters were defined: a 0.25 mm gap between the plates, controlled temperature of 25 °C, and an angular deformation rate of 0.01 rad/s over a period of 240 seconds. Choosing a low shear rate during the analysis was crucial to ensure that the deformation process did not interfere with the viscosity response of the material.

RESULTS

Molecular Modeling & Docking

The results of dermatan sulphate docking using the modeled apo-B100, permitted the prediction of interactions that may be important in the binding process. The ligand formed mainly hydrogen bond with residues S(serine)3343, K(lysine)3345, S(serine)3346, R(arginine)3392 and N(asparagine)3421. An ionic interaction between dermatan sulphate carboxyl oxygen and amidine nitrogen of R3392 was also predicted (**Figure 1**), where Nitrogen atoms are shown in

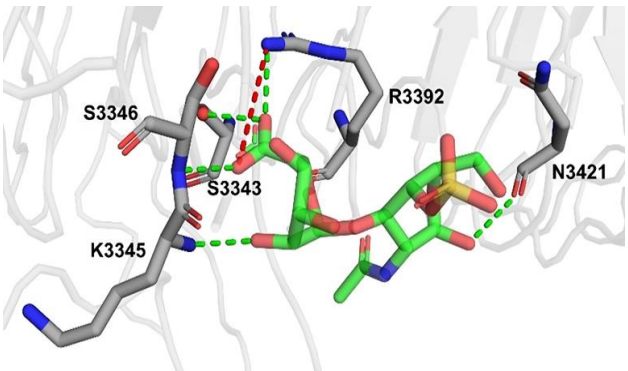

Figure 1. Best docking pose of dermatan sulphate & predicted interactions with apo-B100 modeled structure (Source: Authors' own elaboration)

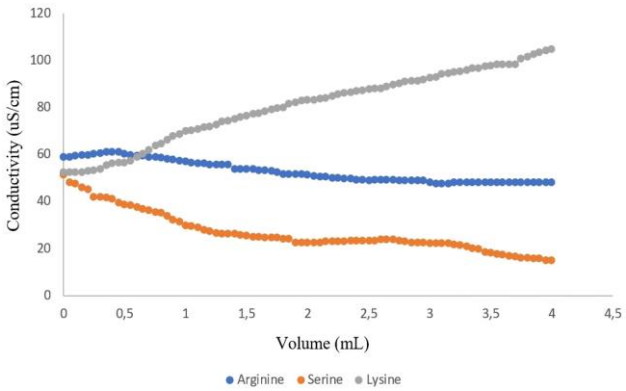

Figure 2. Conductimetric titration: Carrageenan & amino acids (Source: Authors' own elaboration)

blue, oxygen atoms in red, carbon atoms in gray (protein) or green (ligand), hydrogens were omitted for clarity. Molecular interactions are shown as dotted lines: hydrogen bonds in green and ionic interactions in red.

Conductimetric Titration

Figure 2 shows the conductimetric titration curves of carrageenan polymeric solution with titrants, specifically lysine, arginine, and serine solutions. The conductance curve of lysine exhibits an increasing trend, whereas the curves for arginine and serine demonstrate remarkably similar decreasing values.

Figure 2 describes the conductometric curves of amino acids: the increasing curve of lysine is depicted in gray, the decreasing curve of arginine in blue, and the decreasing curve of serine in orange.

Chemical Characterization by FTIR

FTIR spectra of carrageenan, amino acids, and carrageenan-amino acid samples are shown in **Figure 3**. The carrageenan spectrum shows a broad absorption band at 3,380 cm^{-1} attributed to the axial deformation of OH groups and an absorption band at 1,050 cm^{-1} corresponding to O=S=O bonds. The absorption band at 1630 cm^{-1} corresponds to the angular deformation of OH groups from residual water molecules present in the polysaccharide [66]. The lysine spectrum displays double strong bands at 1,620 cm^{-1} and 1,558 cm^{-1} typical of the stretching of COO^- and the stretching and bending vibrations of NH bonds, respectively [67]. The carrageenan-lysine mixture spectrum shows a shift in the band

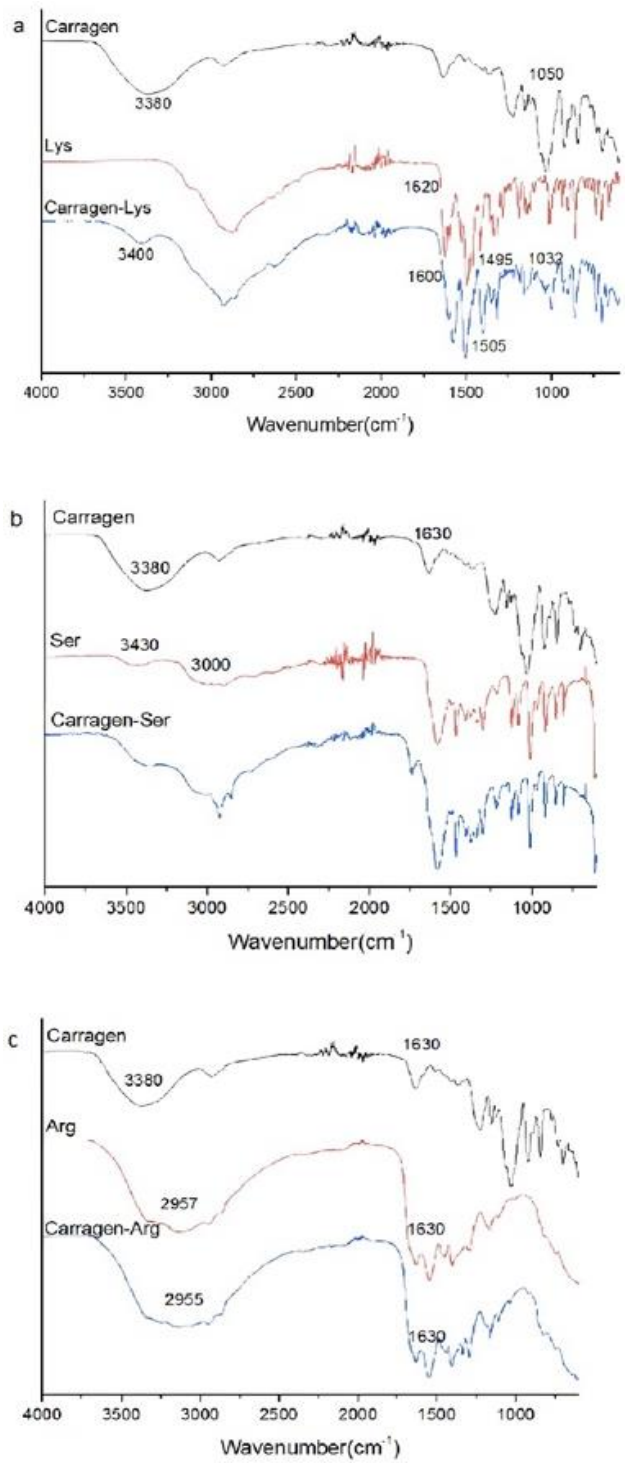

Figure 3. FTIR spectrum-carrageenan, amino acid, & carrageenan-amino acids: (a) FTIR spectrum in blue carrageenan bands, in black lysine bands, in red carrageenan-lysine bands; (b) FTIR spectrum in black carrageenan bands, in red serine bands, in blue carrageenan-serine bands; & (c) FTIR spectrum in black carrageenan bands, in red arginine bands, in blue carrageenan-arginine bands (Source: Authors' own elaboration)

at 3,380 cm^{-1} to 3,400 cm^{-1}, indicating the interaction of the polymer with the amino acid via the OH groups from carrageen.

The analysis also indicates the shift of the band related to the axial deformation of COO^- at 1,620 cm^{-1} in the amino acid to 1,600 cm^{-1} in the mixture, and the shift of the NH bending

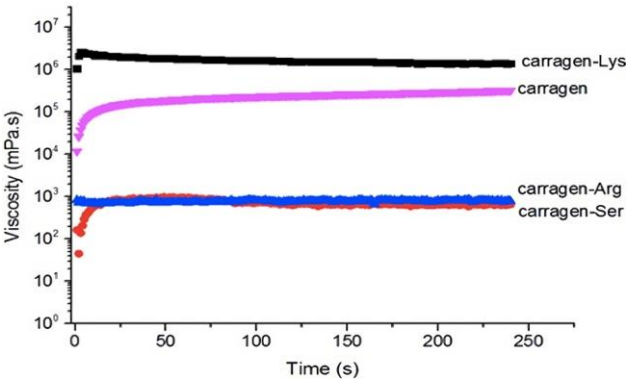

Figure 4. Rheological results of the viscosities of carrageenan, carrageenan-lysine, carrageenan-arginine, & carrageenan-serine (Source: Authors' own elaboration)

from 1,495 cm^{-1} on the amino acid to 1,505 cm^{-1} on the mixture [68]. These band shifts in the carrageenan-lysine spectrum indicate the molecular interaction between the polymer and the amino acid.

This result is in total agreement with the theoretical model in which the OH from the carrageen polymer (showed in green in the model), interacts with the amino group from lysine (K3345) by hydrogen bond.

The serine spectrum showed an absorption bands at 3,430 cm^{-1} attributed to the axial deformation of NH_2, at 3,000 cm^{-1} attributed to the stretching of the OH of carboxylic acid [69], and its typical fingerprinting bands, below 1,100 cm^{-1}.

The carrageenan-serine mixture spectrum shows absorption bands at 3,430 cm^{-1}, 3,196 cm^{-1}, and at 2,940 cm^{-1} [68], indicating the overlapping of the amino acid and carrageen bands at this region. These results suggest no molecular interaction between the polymer and the amino acid.

Typical stretching frequencies of arginine are NH bond of the amine at 2,957 cm^{-1} and C=O of the carboxyl group at 1,630 cm^{-1} [70]. The carrageenan–arginine spectrum did not show shifts when compared to the polymer or the isolated amino acid. The resulting spectra is the overlapping of the polymer and the amino acid spectrum, indicating no molecular interaction.

Rheology

Figure 4 shows the viscosity of the analyzed samples, including carrageenan, carrageenan-lysine, carrageenan-arginine, and carrageenan-serine, where viscosity curves in lilac carrageenan polymer, in black carrageenan-lysine solution, in blue carrageenan-arginine solution, in red carrageenan-serine solution.

Viscosities remained relatively constant during the analysis. Comparing the viscosity of carrageenan with the viscosities of carrageenan-amino acid mixtures, it was observed that the viscosity of the carrageenan-lysine sample exceeded the viscosities of the polymer and the carrageenan-arginine or carrageenan-serine samples, indicating a greater molecular interaction between lysine and the polymer.

Figure 5 displays the photographs of the carrageenan, amino acids, and carrageenan-amino acid solutions before the rheological analysis. The formation of a gel-like precipitate in the carrageenan-lysine sample is evident.

Figure 5. Samples of carrageenan, amino acids, & carrageenan-amino acid solutions: (a) Carrageenan solution, lysine solution, & carrageenan-lysine solution; (b) carrageenan solution, arginine solution, & carrageenan-arginine solution; & (c) carrageenan solution, serine solution, & carrageenan-serine solution (Source: Authors' own elaboration)

Figure 5 describes the physical state of the solutions used in rheological analysis, in sequence: polymeric solution, amino acid solution and polymer-amino acid solution.

DISCUSSION

Since there are no solved structures for apo-B100, our results originate a model, which may help to understand dermatan sulphate interactions with the referred protein. It is important to notice that it does not show the mechanism of action but brings insights on how they may work.

To better understand the process, it would be necessary to elucidate protein structure, which is a difficult task, based on its mass and complexity. In this sense, our model was constructed based on a small sequence of 355 amino acids, therefore, it does not represent the full structure of the protein. The amino acids sequence was chosen according to [38], which identified as apo-B100 binding site for proteoglycans.

Although it is a small model, we found that the main interactions occur in accordance with previous results in other works. In fact, the results show interactions with L (leucine) residue by hydrogen bond and that other residues such as S (serine), R (arginine), K (lysine) and N (asparagine) seem important for ligand/protein interaction.

Another important finding is the predicted electrostatic interaction between R (arginine) and dermatan sulphate, showing the importance of positive interaction in ligand target bonding [38]. In spite of predicting important interactions the biding region was modelled similar to random coils, which may influence docking results.

For instance, L (leucine) 3391, a known important residue did not show interactions with dermatan sulphate. On the other hand, the model was able to predict possible mechanisms of interactions, considering the characteristics of

amino acid residues and dermatan sulphate. The apolipoprotein B-100 molecule contains 4.536 amino acid residues with several interaction sites.

It was explored some of these sites found that the site composed by the 3359- 3369 residues, specifically the amino acids arginine 3362, lysine 3363, and arginine 3364 can promote the interactions between LDL molecules and the glycosaminoglycans from the arterial endothelial tissue [38]. When replacing these amino acids by acidic amino acids such as glutamic acid or aspartic acid, the interaction of LDL molecules with glycosaminoglycans was disrupted, mainly when the lysine residue 3363 was replaced by glutamic acid [38]. Based on these studies, a computational model was designed here, to investigate the amino acids involved in the molecular interaction process that starts the plaque formation in the arterial vessels tissues, namely, the adhesion of the lipids (from LDL) to the epithelial tissues.

The experimental investigation was carried out using the carrageenan polymer, as it displays sulfated groups and free hydroxyls in its molecular structure, and the absence of carboxyl groups. The tested amino acids were lysine, arginine, and serine, present at the surface of the apolipoprotein B-100 molecule, as suggested by the computational model.

In summary, the literature describes that in lesions in injured arterial endothelial tissues, the immune system cells express the glycosaminoglycans (dermatan sulfate and chondroitin sulfate) on their surface [71, 72]. These molecules have negative charges in their structure, which are available on the surface of arterial endothelial cells, forming a high-density network of negative charges. Our results suggest that these negative charges attract LDL molecules to the injured region, initiating the adhesion process of LDL to the endothelial tissue. Electrostatic attraction occurs between the electronegative groups present in the glycosaminoglycan molecules of endothelial tissue and the electropositive amino acid residues on the surface of apolipoprotein B-100 molecules of LDL.

Regarding the carrageenan solution, it is highly stable under neutral or alkaline pH [73]. The conductimetric titration experiment was carried out at pH 7, close to the physiological environment (pH 7.4). At this pH, carrageenan is negatively charged, its sulphate and hydroxyl groups are both deprotonated. Lysine displays a secondary amino group in its side chain and a secondary amino group in its main chain, both protonated at pH 7. Its hydroxyl group is deprotonated. Arginine, featuring a guanidinium group, displays ionizable side chains in its molecular structure, from its protonated amine and deprotonated hydroxyl group. Serine displays one protonated amine and one deprotonated hydroxyl group [74]. These features may have an important role in interactions between dermatan sulphate and apo B-100.

The conductimetric titration of carrageenan with lysine showed an ascending curve, which may be attributed to the increase in ions available in solution arising from the positive charge of the lysine's structure. At the beginning, the curve shows a stable profile, followed by an increase in conductivity as the result of the addition of lysine. This result can be correlated to the neutralization of the carrageenan hydroxyl groups by free lysine amine groups, followed by the excess of free amine in solution, resulting in increased conductivity [75].

The conductimetric titration curve of carrageenan with arginine or serine displayed a very similar behavior, with a slightly decrease in the conductivity values. The guanidine side chain from arginine provide a positive delocalized charge, resulting from its conjugated system between double bonds and hydrogen atoms [76]. The system's conductance decreases because the molecular interactions of the terminal amine group of arginine and the negative charges from the polymer, with no excess of positive charges. This behavior is similar for serine in which its single amine protonated group interacts with the negative charges from the polymer, and no excess of positive charges. In these cases, the positive charges (amino group) was mobilized to neutralize the polymer's charges, and the negative charge (hydroxyl), which did not interact with the polymer was responsible for the system's conductivity.

As shown in **Figure 4** and **Figure 5**, the mixture of carrageenan with amino acids leads to interesting results, mainly the formation of a gel when mixing carrageenan with lysine, and the break of the viscous state of carrageenan when mixing with arginine or serine. Viscosity is directly associated with molecular interactions; the greater the intermolecular forces, the higher the viscosity of the system [77]. Several natural systems are formed and structured by electrostatic complexes between proteins and polysaccharides. The interactions of these systems depend on the electric charges of the polymers, pH, and ionic strength. They can be incompatible or compatible [78]. Incompatible interactions between similarly charged molecules, result in electrostatic repulsion [78]. Compatible interactions result from attraction between molecules with opposite electric charges. Compatibility interactions occur in a pH range located between the protein's isoelectric point (pI) and the polysaccharide's pKa. Under these conditions, molecules are attracted to each other, leading to the formation of precipitates [78], such as gels [79]. In these gels, the interaction force is proportional to the number of charged groups; the more charged molecules, the stronger the precipitates, and the ionic strength of the mixture influences gel stability [80]. The nature of the electrically charged group also influences the strength of interactions. Certain proteins interact more strongly with polysaccharides containing sulfonic groups than polysaccharides with only carboxylic groups [77]. Most proteins have some lysine residues; the amino groups of lysine are usually exposed on the protein's surface and are highly reactive when protonated. The high reactivity of carrageenan with lysine is due to the strong electrostatic interaction between the negatively charged groups of carrageenan and the positively charged side chain of lysine. Interactions between carrageenan and lysine can be observed by the gelation of the solution [77]. Arginine has a guanidine group and an end terminal amine group, which carries a positive charge under physiological conditions because of their intrinsic pKa; although the guanidine group is protonated, its positive charge is delocalized due to the presence of the conjugated double bonds between carbon and nitrogen atoms [68]. Thus, the moderate interaction between arginine and carrageenan is attributed to the guanidinium group in the amino acid's side chain, which has six π electrons in bonding orbitals and is protonated with a positively charged delocalized form at neutral pH [76]. Serine is a neutral amino acid and its interaction with carrageenan is the result of the interaction of its only amine end group with the negative charges of polymer [76]. All these data are in total agreement with FTIR results and with the proposed theoretical model.

The results and the proposal of this adhesion model are described here for the first time, to the best of our knowledge. It is a preliminary proposal, however it shows important

results, obtained from simple experiments, that can be useful to future studies and aim to present the issue to the scientific community and sparking interest, encouraging the development of more in-depth studies.

CONCLUSIONS

Herein we presented experimental results aligned with a theoretical model of interaction, using the carrageenan molecule, due to its similarity to dermatan sulfate and amino acids, specifically those present on the surface of apolipoprotein B-100 molecules.

The results of the conductometric titration, with carrageenan as the titrated polymer and lysine, arginine, and serine as titrants, showed that all three amino acids interacted with the polymer. The rising titration curve of lysine demonstrated a greater availability and mobility of lysine ions in the system. Rheological analysis addressed molecular interactions through viscosity. All three amino acid solutions showed interaction with carrageenan, and the formation of a gelatinous precipitate in the carrageenan-lysine solution highlighted a greater molecular interaction of lysine with the polymer. FTIR analysis depicted the polymer-amino acid interaction through band shifts, visible in all three spectra. These analyses indicated that among the investigated amino acids, lysine exhibited a greater molecular affinity with the polymer.

The results support the hypotheses addressed in the theoretical model of lipid adhesion, suggesting that the molecular interaction between LDL molecules and the injured vascular tissue occurs through lysine residues present in apolipoprotein B-100. Based on the findings outlined in this study, it is anticipated that these results may help the development of further research projects aimed at advancing in this particular matter. It is also expected that this lipid adhesion model will assist in the development of new drugs, devices, and effective technologies for the control and prevention of atherosclerotic pathologies; reflecting a reduction in atherosclerotic cases, as well as a decrease in mortality rates and sequelae caused by these diseases.

Author contributions: PMCP: research protocol design, literature search, data extraction, draft manuscript, & data interpretation; **TAS & AMG:** analysis, interpretation, draft manuscript, & data interpretation; & **ET:** conception & design, acquisition, analysis, interpretation, draft manuscript, & data interpretation. All authors have agreed with the results and conclusions.

Funding: This study was supported by São Paulo Research Foundation under Grant 2017/18782-6.

Ethical statement: The authors stated that the study did not involve testing on animals/humans. The authors further stated that approval by an ethics committee was not required for the study.

Declaration of interest: No conflict of interest is declared by the authors.

Data sharing statement: Data supporting the findings and conclusions are available upon request from the corresponding author.

REFERENCES

1. Benslaiman S, Galicia-García U, Larrea-Sebal A, et al. Pathophysiology of atherosclerosis. Int J Mol Sci. 2022;23(6):3346. https://doi.org/10.3390/ijms23063346 PMid:35328769 PMCid:PMC8954705
2. Sumida K, Molnar MZ, Potukuchi PK, et al. Constipation and risk of death and cardiovascular events. Atherosclerosis. 2018;281:114-20. https://doi.org/10.1016/j.atherosclerosis.2018.12.021 PMid:30658186 PMCid:PMC6399019
3. Gimbrone Jr MA, García-Cardeña G. Endothelial cell dysfunction and the pathobiology of atherosclerosis. Circ Res. 2016;118(4):620-36. https://doi.org/10.1161/CIRCRESAHA.115.306301 PMid:26892962 PMCid:PMC4762052
4. Norlund F, Lissåker C, Wallert J, Held C, Olsson EM. Factors associated with emotional distress in patients with myocardial infarction: Results from the SWEDEHEART registry. Eur J Prev Cardiol. 2018;25(9):910-20. https://doi.org/10.1177/2047487318770510 PMid:29692223 PMCid:PMC6009178
5. Poledne R, Kovar J. Hypertriglyceridemie a riziko aterosklerozy. Vnitřní Lékařství. 2019;65(12):783-7. https://doi.org/10.36290/vnl.2019.136
6. Bentzon JF, Otsuka F, Virmani R, Falk E. Mechanisms of plaque formation and rupture. Circ Res. 2014;114(12):1852-66. https://doi.org/10.1161/CIRCRESAHA.114.302721 PMid:24902970
7. Mohanta SK, Yin C, Peng L, et al. Artery tertiary lymphoid organs contribute to innate and adaptive immune responses in advanced mouse atherosclerosis. Circ Res. 2014;114(11):1772-87. https://doi.org/10.1161/CIRCRESAHA.114.301137 PMid:24855201
8. Libby P. The changing landscape of atherosclerosis. Nature. 2021;592(7855):524-33. https://doi.org/10.1038/s41586-021-03392-8 PMid:33883728
9. Gargiulo P, Marsico F, Parente A, et al. Ischemic heart disease in systemic inflammatory diseases. An appraisal. Int J Cardiol. 2014;170(3):286-90. https://doi.org/10.1016/j.ijcard.2013.11.048 PMid:24331863
10. Abdelhamid AS, Brown TJ, Brainard JS, et al. Omega-3 fatty acids for the primary and secondary prevention of cardiovascular disease. Cochrane Database Syst Rev. 2020;29;3(3):CD003177. https://doi.org/10.1002/14651858.CD003177.pub5 PMid:32114706
11. Frostegård J. Immunity, atherosclerosis and cardiovascular disease. BMC Med. 2013;11:117. https://doi.org/10.1186/1741-7015-11-117 PMid:23635324 PMCid:PMC3658954
12. Roth GA, Abate D, Abate KH, GBD 2017 Causes of Death Collaborators. Global, regional, and national age-sexspecific mortality for 282 causes of death in 195 countries and territories, 1980-2017: A systematic analysis for the global burden of disease study 2017. Lancet. 2018;392(10159):1736-88. https://doi.org/10.1016/S0140-6736(18)32203-7 PMid:30496103
13. Brant LCC, Nascimento BR, Passos VMA, et al. Variations and particularities in cardiovascular disease mortality in Brazil and Brazilian states in 1990 and 2015: Estimates from the global burden of disease. Rev Bras Epidemiol. 2017;01(01):116-28. https://doi.org/10.1590/1980-5497201700050010 PMid:28658377
14. Reed GW, Rossi JE, Cannon CP. Acute myocardial infarction. Lancet. 2022;389(10065):197-210. https://doi.org/10.1016/S0140-6736(16)30677-8 PMid:27502078
15. Avezum JA, Feldman A, Carvalho ACC, et al. V guideline of the Brazilian Society of Cardiology on acute myocardial infarction treatment with ST segment elevation. Arq Bras Cardiol. 2015;105(2Suppl 1):1-105.

16. Faria-Fortini I, Basílio ML, Scianni AA, Faria CDCM, Teixeira-Salmela LF. Performance and capacity-based measures of locomotion, compared to impairment-based measures, best predicted participation in individuals with hemiparesis due to stroke. Disabil Rehabil. 2018;40:1791-8. https://doi.org/10.1080/09638288.2017.1312570 PMid: 28395524
17. Tadi P, Lui F. Acute stroke. Treasure Island, FL: StatPearls Publishing; 2024.
18. Powers WJ, Rabinstein AA, Ackerson T, et al. Guidelines for the early management of patients with acute ischemic stroke: 2019 update to the 2018 guidelines for the early management of acute ischemic stroke a guideline for healthcare professionals from the American Heart Association/American Stroke Association. Stroke. 2019;50(12):344-418. https://doi.org/10.1161/STR.0000000000000211 PMid:31662037
19. Rolim D, Sampaio S, Dias PG, Almeida P, Lopes JA, Teixeira JF. Mortality after amputation. Journal Angiologia e Cirurgia Vascular. 2015;11(3):166-70. https://doi.org/10.1016/j.ancv.2015.06.001
20. Tabas I, Garcia- Cardeña, G, Owens GK. Recent insights into the cellular biology of atherosclerosis. J Cell Biol. 2015;209(1):13-22. https://doi.org/10.1083/jcb.201412052 PMid:25869663 PMCid:PMC4395483
21. Geovanini GR, Libby P. Atherosclerosis and inflammation: overview and updates. Clin Sci (Lond). 2018;132(12):1243-52. https://doi.org/10.1042/CS20180306 PMid:29930142
22. Harris WS, Tintle NL, Etherton MR, Vasan RS. Erythrocyte long-chain omega-3 fatty acid levels are inversely associated with mortality and with incident cardiovascular disease: The framingham heart study. J Clin Lipidol. 2018;12(3):718-27.e6. https://doi.org/10.1016/j.jacl.2018.02.010 PMid:29559306 PMCid:PMC6034629
23. Wang HH, Garruti G, Liu M, Portincasa P, Wang DQ. Cholesterol and lipoprotein metabolism and atherosclerosis: Recent advances in reverse cholesterol transport. Ann Hepatol. 2017;16(Suppl. 1:s3-105.):s27-42. https://doi.org/10.5604/01.3001.0010.5495 PMid:29080338
24. Ference BA, Ginsberg HN, Graham I, et al. Low-density lipoproteins cause atherosclerotic cardiovascular disease. Eur Heart J. 2017;38(32):2459-72. https://doi.org/10.1093/eurheartj/ehx144 PMid:28444290 PMCid:PMC5837225
25. Di Fusco SA, Maggioni AP, Scicchitano P, Zuin M, D'Elia E, Colivicchi F. Lipoprotein (a), inflammation, and atherosclerosis. J Clin Med. 2023;12(7):2529. https://doi.org/10.3390/jcm12072529 PMid:37048611 PMCid:PMC10095203
26. Wolf D, Ley K. Immunity and Inflammation in Atherosclerosis. Circ Res. 2019;124(2):315-27. https://doi.org/10.1161/CIRCRESAHA.118.313591 PMid: 30653442 PMCid:PMC6342482
27. Ketelhuth DF, Hansson GK. Adaptive response of T and B cells in atherosclerosis. Circ Res. 2016;118(4):668-78. https://doi.org/10.1161/CIRCRESAHA.115.306427 PMid: 26892965
28. McCarthy CG, Goulopoulou S, Wenceslau CF, Spitler K, Matsumoto T, Webb RC. Toll-like receptors and damage-associated molecular patterns: Novel links between inflammation and hypertension. Am J Physiol Heart Circ Physiol. 2014;306(2):H184-196. https://doi.org/10.1152/ajpheart.00328.2013 PMid:24163075 PMCid:PMC3920129
29. Di Pietro N, Formoso G, Pandolfi A. Physiology and pathophysiology of oxLDL uptake by vascular wall cells in atherosclerosis. Vascul Pharmacol. 2016;84:1-7. https://doi.org/10.1016/j.vph.2016.05.013 PMid:27256928
30. Dower JI, Geleijnse JM, Gijsbers L, Schalkwijk C, Kromhout D, Hollman PC. Supplementation of the pure flavonoids epicatechin and quercetin affects some biomarkers of endothelial dysfunction and inflammation in (pre)hypertensive adults: A randomized double-blind, placebo-controlled, crossover trial. J Nutr. 2015; 145(7):1459-63. https://doi.org/10.3945/jn.115.211888 PMid:25972527
31. Rojas J, Salazar J, Martínez MS, et al. Macrophage heterogeneity and plasticity: Impact of macrophage biomarkers on atherosclerosis. Scientifica (Cairo). 2015;2015:851252. https://doi.org/10.1155/2015/851252 PMid:26491604 PMCid:PMC4600540
32. Zhu Y, Xian X, Wang Z, et al. Research progress on the relationship between atherosclerosis and inflammation. Biomolecules. 2018;8(3):80. https://doi.org/10.3390/biom8030080 PMid:30142970 PMCid:PMC6163673
33. Fan J, Watanabe T. Atherosclerosis: Known and unknown. Pathol Int. 2022;72(3):151-60. https://doi.org/10.1111/pin.13202 PMid:35076127
34. Hilgendorf I, Swirski FK. Making a difference: Monocyte heterogeneity in cardiovascular disease. Curr Atheroscler Rep. 2012;14(5):450-9. https://doi.org/10.1007/s11883-012-0274-8 PMid:22847772 PMCid:PMC3436972
35. Lichtman AH, Binder CJ, Tsimikas S, Witztum JL. Adaptive immunity in atherogenesis: New insights and therapeutic approaches. J Clin Invest. 2013;123(1):27-36. https://doi.org/10.1172/JCI63108 PMid:23281407 PMCid: PMC3533280
36. Suzuki J, Hamada E, Shodai T, et al. Cytokine secretion from human monocytes potentiated by p-selectin-mediated cell adhesion. Int Arch Allergy Appl Immunol. 2013; 160(2):152-60. https://doi.org/10.1159/000339857 PMid:23018521
37. Paoletti R, Bolego C, Poli A, Cignarella A. Metabolic syndrome, inflammation and atherosclerosis. Vasc Health Risk Manag. 2006;2(2):145-52. https://doi.org/10.2147/vhrm.2006.2.2.145 PMid:17319458 PMCid:PMC1993992
38. Borén J, Williams KJ. The central role of arterial retention of cholesterol-rich apolipoprotein-B-containing lipoproteins in the pathogenesis of atherosclerosis: A triumph of simplicity. Curr Opin Lipidol. 2016;27(5):473-83. https://doi.org/10.1097/MOL.0000000000000330 PMid: 27472409
39. Bertassoni LE, Swain MV. The contribution of proteoglycans to the mechanical behavior of mineralized tissues. J Mech Behav Biomed Mater. 2014;38:91-104. https://doi.org/10.1016/j.jmbbm.2014.06.008 PMid: 25043659
40. Mouw JK, Ou G, Weaver VM. Extracellular matrix assembly: a multiscale deconstruction. Nat Rev Mol Cell Biol. 2014;15(12):771-85. ttps://doi.org/10.1038/nrm3902 PMid: 25370693 PMCid:PMC4682873
41. Kali A, Shetty KS. Endocan: A novel circulating proteoglycan. Indian J Pharmacol. 2014;46(6):579-83. https://doi.org/10.4103/0253-7613.144891 PMid:25538326 PMCid:PMC4264070

42. Sakakura K, Nakano M, Otsuka F, Ladich E, Kolodgie FD, Virmani R. Pathophysiology of atherosclerosis plaque progression. Heart Lung Circ. 2013;22(6):399-411. https://doi.org/10.1016/j.hlc.2013.03.001 PMid:23541627
43. Subbotin VM. Excessive intimal hyperplasia in human coronary arteries before intimal lipid depositions is the initiation of coronary atherosclerosis and constitutes a therapeutic target. Drug Discov Today. 2016;21(10):1578-95. https://doi.org/10.1016/j.drudis.2016.05.017 PMid:27265770
44. Fogelstrand P, Borén J. Retention of atherogenic lipoproteins in the artery wall and its role in atherogenesis. Nutr Metab Cardiovasc Dis. 2012;22(1):1-7. https://doi.org/10.1016/j.numecd.2011.09.007 PMid:22176921
45. Neufeld EB, Zadrozny LM, Phillips D, Aponte A, Yu ZX, Balaban RS. Decorin and biglycan retain LDL in disease-prone valvular and aortic subendothelial intimal matrix. Atherosclerosis. 2014;233(1):113-21. https://doi.org/10.1016/j.atherosclerosis.2013.12.038 PMid:24529131 PMCid:PMC3952492
46. Yurdagul A Jr, Finney AC, Woolard MD, Orr AW. The arterial microenvironment: The where and why of atherosclerosis. Biochem J. 2016;473(10):1281-95. https://doi.org/10.1042/BJ20150844 PMid:27208212 PMCid:PMC5410666
47. Yang X, Li Y, Ren X, et al. Oxidative stress-mediated atherosclerosis: Mechanisms and therapies. Front Physiol. 2017;8:600. https://doi.org/10.3389/fphys.2017.00600 PMid:28878685 PMCid:PMC5572357
48. Ammirati E, Moroni F, Magnoni M, Camici PG. The role of T and B cells in human atherosclerosis and atherothrombosis. Clin Exp Immunol. 2015;179(2):173-87. https://doi.org/10.1111/cei.12477 PMid:25352024 PMCid:PMC4298395
49. Yurdagul A Jr, Green J, Albert P, McInnis MC, Mazar AP, Orr AW. α5β1 integrin signaling mediates oxidized low-density lipoprotein-induced inflammation and early atherosclerosis. Arterioscler Thromb Vasc Biol. 2014;34(7):1362-73. https://doi.org/10.1161/ATVBAHA.114.303863 PMid:24833794 PMCid:PMC4096780
50. Mitra S, Deshmukh A, Sachdeva R, Lu J, Mehta JL. Oxidized low-density lipoprotein and atherosclerosis implications in antioxidant therapy. Am J Med Sci. 2011;342(2):135-42. https://doi.org/10.1097/MAJ.0b013e318224a147 PMid:21747278
51. Gisterå A, Hansson G. The immunology of atherosclerosis. Nat Rev Nephrol. 2017;13:368-80. https://doi.org/10.1038/nrneph.2017.51 PMid:28392564
52. Ziegler T, Abdel Rahman F, Jurisch V, Kupatt C. Atherosclerosis and the capillary network: Pathophysiology and potential therapeutic strategies. Cells. 2019;9(1):50. https://doi.org/10.3390/cells9010050 PMid:31878229 PMCid:PMC7016600
53. Legein B, Temmerman L, Biessen EA, Lutgens E. Inflammation and immune system interactions in atherosclerosis. Cell Mol Life Sci. 2013;70(20):3847-69. https://doi.org/10.1007/s00018-013-1289-1 PMid:23430000
54. McLaren JE, Michael DR, Ashlin TG, Ramji DP. Cytokines, macrophage lipid metabolism and foam cells: Implications for cardiovascular disease therapy. Prog Lipid Res. 2011;50(4):331-47. https://doi.org/10.1016/j.plipres.2011.04.002 PMid:21601592
55. Skiba DS, Nosalski R, Mikolajczyk TP, et al. Anti-atherosclerotic effect of the angiotensin 1-7 mimetic AVE0991 is mediated by inhibition of perivascular and plaque inflammation in early atherosclerosis. Br J Pharmacol. 2017;174(22):4055-69. https://doi.org/10.1111/bph.13685 PMid:27935022 PMCid:PMC5659999
56. Angelovich TA, Hearps AC, Jaworowski A. Inflammation-induced foam cell formation in chronic inflammatory disease. Immunol Cell Biol. 2015;93(8):683-93. https://doi.org/10.1038/icb.2015.26 PMid:25753272
57. Rahman MS, Woollard K. Atherosclerosis. Adv Exp Med Biol. 2017;1003:121-44. https://doi.org/10.1007/978-3-319-57613-8_7 PMid:28667557
58. Bennett MR, Sinha S, Owens GK. Vascular smooth muscle cells in atherosclerosis. Circ Res. 2016;118(4):692-702. https://doi.org/10.1161/CIRCRESAHA.115.306361 PMid:26892967 PMCid:PMC4762053
59. Kloc M, Ghobrial RM, Wosik J, Lewicka A, Lewicki S, Kubiak JZ. Macrophage functions in wound healing. J Tissue Eng Regen Med. 2019;13(1):99-109. https://doi.org/10.1002/term.2808 PMid:30445662
60. Bao Z, Li L, Geng Y, et al. Advanced glycation end products induce vascular smooth muscle cell-derived foam cell formation and transdifferentiate to a macrophage-like state. Mediators Inflamm. 2020;7;2020:6850187. https://doi.org/10.1155/2020/6850187 PMid:32831637 PMCid:PMC7428884
61. Maguire EM, Pearce SWA, Xiao Q. Foam cell formation: A new target for fighting atherosclerosis and cardiovascular disease. Vascul Pharmacol. 2019;112:54-71. https://doi.org/10.1016/j.vph.2018.08.002 PMid:30115528
62. Libby P, Buring JE, Badimon L, et al. Atherosclerosis. Nat Rev Dis Primers. 2019;5(1):56. https://doi.org/10.1038/s41572-019-0106-z PMid:31420554
63. Kemmish H, Fasnacht M, Yan L. Fully automated antibody structure prediction using BIOVIA tools: Validation study. PLoS One. 2017;12:e0177923. https://doi.org/10.1371/journal.pone.0177923 PMid:28542300 PMCid:PMC5436848
64. Stewart JJP. Optimization of parameters for semiempirical methods VI: More modifications to the NDDO approximations and re-optimization of parameters. Modeling J Mol. 2013;19(1):1-32. https://doi.org/10.1007/s00894-012-1667-x PMid:23187683 PMCid:PMC3536963
65. Macrae CF, Sovago I, Cottrell SJ, et al. Mercury 4.0: From visualization to analysis, design and prediction. J Appl Cristalizador. 2020;53(1):226-35. https://doi.org/10.1107/S1600576719014092 PMid:32047413 PMCid:PMC6998782
66. Ghani NAA, Othaman R, Ahmad A, Anuar FH, Hassan NH. Impact of purification on iota carrageenan as solid polymer electrolyte. Arab J Chem. 2019;12(3):370-6. https://doi.org/10.1016/j.arabjc.2018.06.008
67. Ebrahiminezhad A, Ghasemi Y, Rasoul-Amini S, Barar J, Davaran S. Preparation of novel magnetic fluorescent nanoparticles using amino acids. Colloids Surf B Biointerfaces. 2013;1(102):534-9. https://doi.org/10.1016/j.colsurfb.2012.08.046 PMid:23104022
68. Bruice PY. Organic chemistry. Upper Saddle River, NJ: Pearson; 2016.
69. McMurry J, Begley T. The organic chemistry of biological pathways. Greenwood Village, CO: Roberts & Company Publishers; 2015.

70. Sahaya RAS, Rajendran S. Inhibition of corrosion of carbon steel in well water by DL-phenylalanine-Zn2+system. J Electrochem Sci Eng. 2012;2(2):91-104. https://doi.org/10.5599/jese.2012.0012
71. Matsuo I, Kimura-Yoshida C. Extracellular distribution of diffusible growth factors controlled by heparan sulfate proteoglycans during mammalian embryogenesis. Philos Trans R Soc Lond B Biol Sci. 2014;369(1657):20130545. https://doi.org/10.1098/rstb.2013.0545 PMid:25349453 PMCid:PMC4216467
72. Neill T, Schaefer L, Iozzo RV. Decoding the matrix: Instructive roles of proteoglycan receptors. Biochemistry. 2015;54(30):4583-98. https://doi.org/10.1021/acs.biochem.5b00653 PMid:26177309 PMCid:PMC4859759
73. Błaszak BB, Gozdecka G, Shyichuk A. Carrageenan as a functional additive in the production of cheese and cheese-like products. Acta Sci Pol Technol Aliment. 2018;17(2):107-16. https://doi.org/10.17306/J.AFS.0550 PMid:29803212
74. Attwood PV. P-N bond protein phosphatases. Biochim Biophys Acta. 2013;1834(1):470-8. https://doi.org/10.1016/j.bbapap.2012.03.001 PMid:22450136
75. Zakaria HM, Shah A, Konieczny M, Hoffmann JA, Nijdam AJ, Reeves ME. Small molecule- and amino acid-induced aggregation of gold nanoparticles. Langmuir. 2013;29(25):7661-73. https://doi.org/10.1021/la400582v PMid:23718319
76. Baynes JW. Medical biochemistry. Netherlands: Elsevier; 2010.
77. Vieira Neto JL, Martins AL, Ataíde CH, Barrozo MAS. Non-Newtonian flows in annuli with variable eccentric motion of the inner tube. Chem Eng Technol. 2012;35(11):1981-8. https://doi.org/10.1002/ceat.201200239
78. Bi X, Xiong W, He J, Ma S, Zhang J, Fang Y, Wu Y. Site-selective and biocompatible growth of polymers from glycan moieties of glycoproteins and living cells. Biomacromolecules. 2021;22(10):4237-43. https://doi.org/10.1021/acs.biomac.1c00792 PMid:34474556
79. Yan JN, Cui XF, Jiang XY, Li L, Sun W, Wu HT. Complex characterization and mechanism of formation of scallop protein hydrolysates (patinopecten yessoensis)/κ-carrageenan/konjac gum compound gels. J Food Sci. 2022;87(7):2953-64. https://doi.org/10.1111/1750-3841.16163 PMid:35686600
80. Wu CL, Li XY, Huang XY, et al. Mechanism of formation and textural properties of a complex gel based on soy glycinine-chitosan complex coacervates: Effects of pH, heat treatment temperature and centrifugation. Int J Biol Macromol. 2024;262(2):130170. https://doi.org/10.1016/j.ijbiomac.2024.130170 PMid:38360225